AD-A104 325 R AND D ASSOCIATES MARINA DEL REY CA F/G 14/2
A GROUND-MOTION DISPLACEMENT GAUGE.(U)
AUG 80 J E WHITENER DNA001-80-C-0069
UNCLASSIFIED RDA-TR-113204-004 DNA-5574T NL

1 OF 1
AD
A104 325

END
DATE
FILMED
10-81
DTIC

(12)

DNA 5574T

A GROUND-MOTION DISPLACEMENT GAUGE

Jack E. Whitener
R & D Associates
P. O. Box 9695
Marina del Rey, California 90291

1 August 1980

Topical Report for Period 5 January 1980—1 August 1980

CONTRACT No. DNA 001-80-C-0069

THIS WORK SPONSORED BY THE DEFENSE NUCLEAR AGENCY
UNDER RDT&E RMSS CODE B310080464 P99QAXDB00157 H2590D.

Prepared for
Director
DEFENSE NUCLEAR AGENCY
Washington, D. C. 20305

UNCLASSIFIED

SECURITY CLASSIFICATION OF THIS PAGE

REPORT DOCUMENTATION PAGE		READ INSTRUCTIONS BEFORE COMPLETING FORM
1. REPORT NUMBER DNA 5574T	2. GOVT ACCESSION NO. AD-A104 325	3. RECIPIENT'S CATALOG NUMBER
4. TITLE (and Subtitle) A GROUND-MOTION DISPLACEMENT GAUGE		5. TYPE OF REPORT & PERIOD COVERED Topical Report for Period 5Jan80-1Aug80
		6. PERFORMING ORG. REPORT NUMBER(s) RDA-TR-113204-004
7. AUTHOR(s) Jack E. Whitener		8. CONTRACT OR GRANT NUMBER(s) DNA 001-80-C-0069
9. PERFORMING ORGANIZATION NAME AND ADDRESS R & D Associates, P. O. Box 9695, Marina del Rey, California, 90291		10. PROGRAM ELEMENT, PROJECT, TASK AREA & WORK UNIT NUMBERS Subtask P99QAXDB001-57
11. CONTROLLING OFFICE NAME AND ADDRESS Director, Defense Nuclear Agency, Washington, D.C. 20305		12. REPORT DATE 1 August 1980
		13. NUMBER OF PAGES 52
14. MONITORING AGENCY NAME & ADDRESS (if different from Controlling Office)		15. SECURITY CLASS. (of this report) UNCLASSIFIED
		15a. DECLASSIFICATION/DOWNGRADING SCHEDULE

16. DISTRIBUTION STATEMENT (of this report)

Approved for public release; distribution unlimited.

17. DISTRIBUTION STATEMENT (of the abstract entered in block 20, if different from report)

18. SUPPLEMENTARY NOTES

This work sponsored by the Defense Nuclear Agency under RDT&E RMSS Code B310080464 P99QAXDB00157 H2590D.

19. KEY WORDS (Continue on reverse side if necessary and identify by block number)

Displacement gauge	Time-of-free-fall
Ground motion	Displacement potential
Particle displacement	Air drag

20. ABSTRACT (Continue on reverse side if necessary and identify by block number)

This report describes a ground-motion displacement gauge and its applications. The gauge concept is based upon the free-fall time of a mass released inside a gauge cannister prior to the onset of ground motion. The time-of-fall of the mass to the cannister bottom during ground displacement, together with the free-fall time for the gauge at rest, uniquely determines the vertical displacement at one time. Simulation of ground displacement by gauge drop tests demonstrated the operating principle.

DD FORM 1473 1 JAN 73

EDITION OF 1 NOV 65 IS OBSOLETE

UNCLASSIFIED

SECURITY CLASSIFICATION OF THIS PAGE

UNCLASSIFIED

SECURITY CLASSIFICATION OF THIS PAGE(*When Data Entered*)

UNCLASSIFIED

SECURITY CLASSIFICATION OF THIS PAGE(*When Data Entered*)

SUMMARY

This report summarizes the concept, applications, and results of developmental tests for a special ground-motion displacement gauge. Other possible uses, which have not been tested, are also discussed.

The gauge concept is based upon the free-fall time of a mass released inside a gauge cannister prior to the onset of ground motion. The time-of-fall of the mass to the cannister bottom during ground displacement, together with the free-fall time for the gauge at rest, uniquely determines the vertical displacement at one time. Simulation of ground displacement by gauge drop tests demonstrated the operating principle.

One application of the gauge, for which it was originally proposed, would be to measure permanent displacements produced by underground explosions. The displacement potential determined from the measurement would provide a source strength of seismic signals from the explosion. Another use is to verify the measurements of ground displacement obtained by integration of particle velocity or acceleration gauge data. The size of the gauge is one limiting factor on the range of displacement which can be measured. Another is the ground stress which the gauge must survive. The practical range of measurements would be from .1- to 100-cm displacement.

PREFACE

This report describes a ground-motion displacement gauge previously proposed by RDA. Publication of the report was prompted by suggestions from Mr. R. J. Port of RDA for new applications in high-explosive simulation programs. Dr. E. A. Martinelli offered valuable assistance on other applications discussed in the report.

TABLE OF CONTENTS

TABLE OF CONTENTS (CONCLUDED)

LIST OF ILLUSTRATIONS

LIST OF TABLES

I. INTRODUCTION

This report describes the concept and development of a ground-motion displacement gauge suggested by the author at RDA in 1972 (Ref. 1). During the period 1972 through 1973, the MIGHTY MITE series of nuclear and high-explosive underground tests were conducted at the Nevada Test Site. The objective of these tests was to determine the effectiveness of various heat sink concepts for quenching explosions inside cavities. The Advanced Research Projects Agency (ARPA) sponsored the test program which was executed by the Defense Nuclear Agency. ARPA was primarily concerned that, in the event of complete test ban negotiations, clandestine tests in underground cavities could deny seismic detection. Reference 2 describes these tests.

From the theory of cavity decoupling, it has been shown that the seismic energy transmitted to teleseismic distances ($\sim 10^3$ km) is related to the permanent elastic particle displacement at or near the cavity wall (Ref. 3).

In Appendix A a derivation is given for the relation between permanent displacement and the energy released in a cavity. This application of a permanent ground-motion displacement measurement motivated the concept of the gauge discussed in this report.

II. DESCRIPTION OF THE VERTICAL DISPLACEMENT GAUGE

1. OPERATING PRINCIPLE

The principle of gauge operation is illustrated using Figures 1 and 2. In Figure 1, the initial position of the gauge case is shown in the solid figure. Any point A of the gauge case moves to a new position B along the displacement path. At time prior to the beginning of motion, a mass is released at the top of the gauge. On impact of the mass shorting pin upon the foil switch located at the bottom of the gauge case, the time of impact is recorded with the gauge now at position B. During the time-of-fall, the mass drops through the distance ℓ and the gauge is displaced vertically by the amount d as shown. For the case of no vertical motion, the mass would drop a fixed distance S as shown in Figure 1. From the recorded release and impact times, t_r and t_i respectively, the displacement is determined by

$$d = S - 1/2g(t_i - t_r)^2$$

or alternatively,

$$d = 1/2g \left\{ t_o^2 - (t_i - t_r)^2 \right\} \qquad (1)$$

where

$$S = 1/2gt_o^2 \qquad (2)$$

and t_o is the drop time for zero displacement. If $t_i - t_r > t_o$, the displacement is downward. If $t_i - t_r < t_o$, the motion is upward.

It is emphasized that so far this gauge design measures only vertical displacement at just one point.

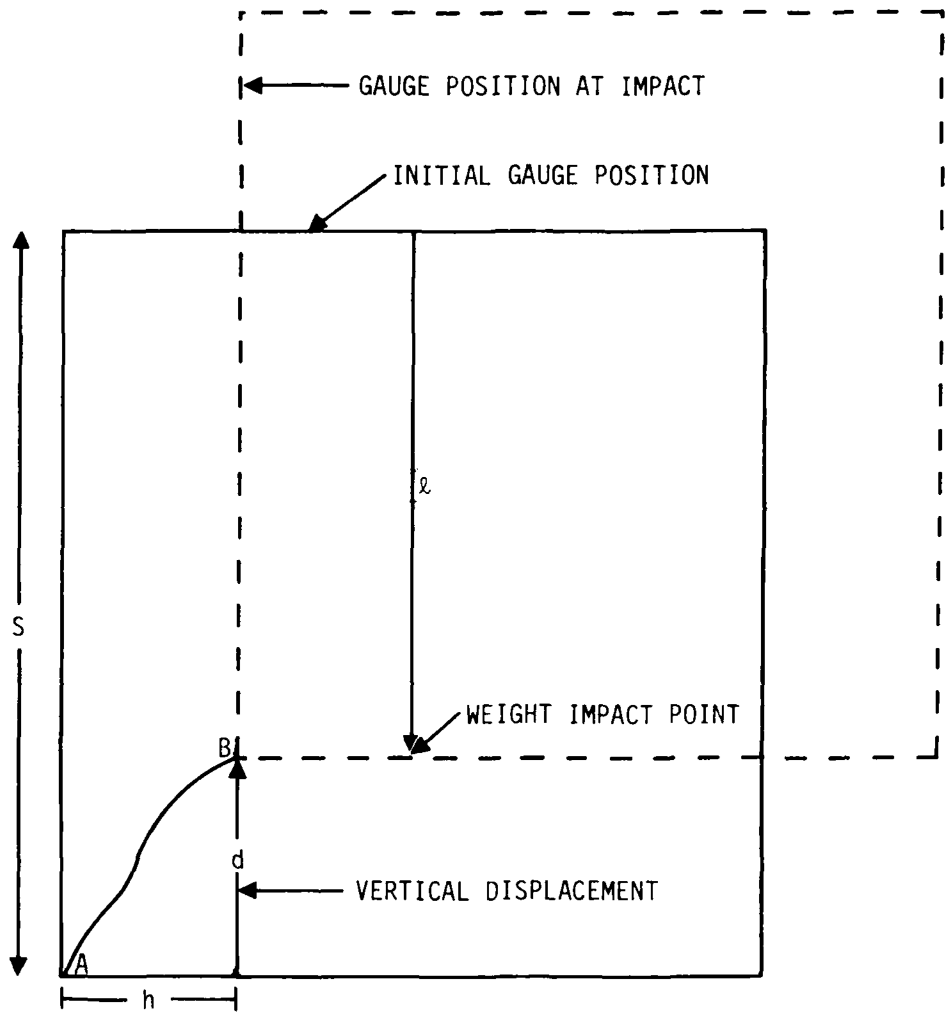

Figure 1. Principle of ground-motion gauge operation.

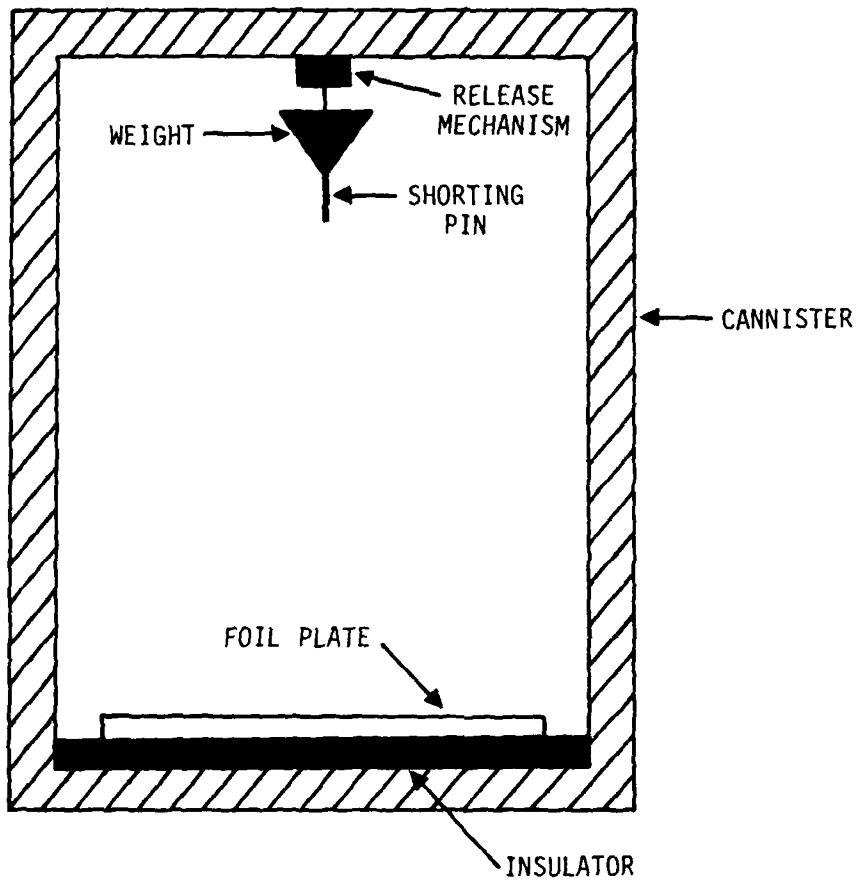

Figure 2. Schematic showing basic components of ground-motion displacement gauge.

2. OPERATIONAL CONSTRAINTS

Several features of this technique may limit the application of the gauge to a specific range of displacement measurements. Gauge construction must be preceded by careful estimates of the maximum motions and durations expected.

a. Gauge dimensions

(1) Upward displacement--The maximum upward displacement which can be measured must be less than S, otherwise the weight impact would occur prior to the peak value of displacement. Thus the vertical dimensions must be greater than $1/2gt_o^2$. Figure 3 shows a plot of Eq. 2 to estimate the gauge size S. It is noted that the gauge size rapidly increases with the time-of-fall for upward motions.

In Figure 4, two upward-displacement waveforms are shown corresponding to a cube-root yield scaling factor of 2. The dashed curves are the free-fall paths for the different gauge sizes shown and for zero time of release. A mass drop height of almost 8 cm is required to measure displacement beyond the peak for W = 1, while about 4 cm is required for the smaller waveform. For smaller drop heights S, impact occurs prior to the peak displacement. It can also be noted that the gauge size S does not scale with $W^{1/3}$ since the time-of-fall of the weight does not scale.

Another parameter which could be useful is controlled advance or delay time-of-weight release. Figure 5 illustrates these effects of advance or delay in the release time relative to zero time of release for upward displacement. The figure shows the different impact times for releases at -15 and +15 ms for 2.54-cm and 5-cm gauge sizes.

(2) Downward displacement--Downward displacements present different problems since the gauge motion is following the free-fall of the weight. The downward displacement

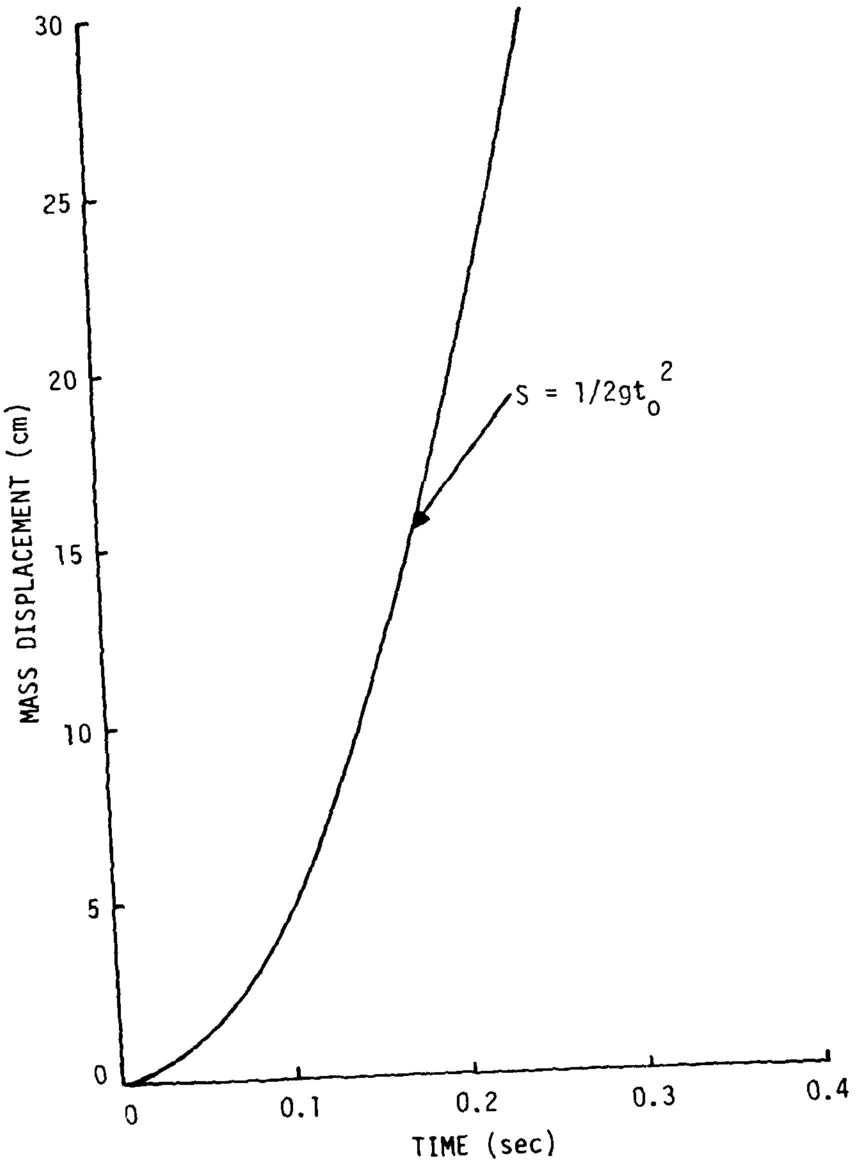

Figure 3. Estimate of gauge size vs zero-displacement drop time.

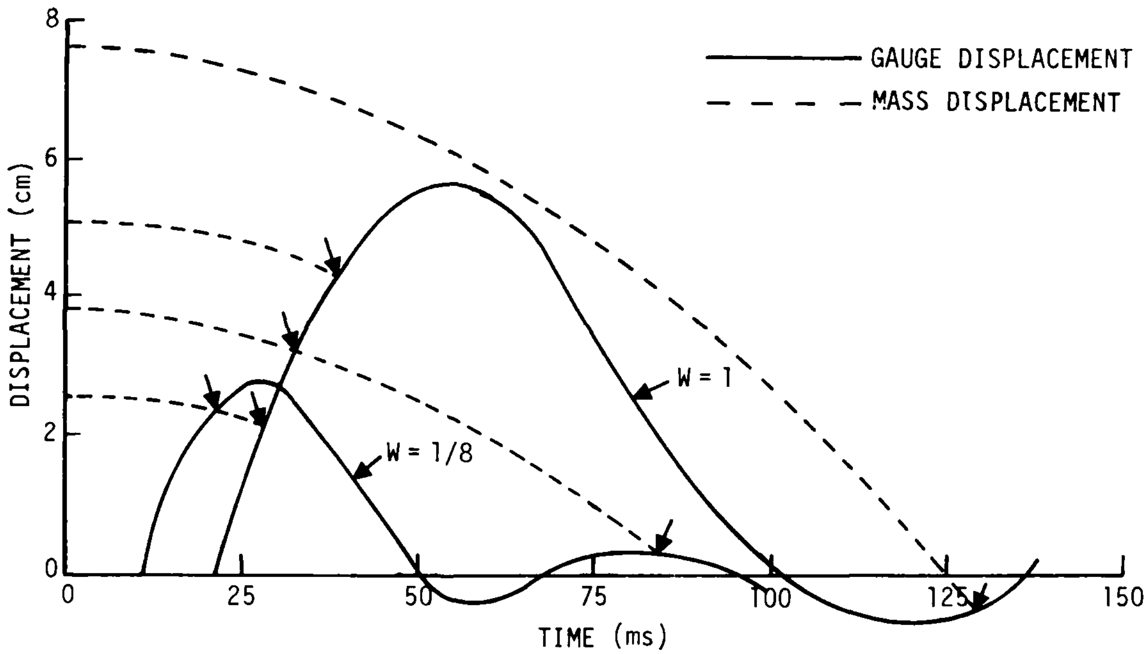

Figure 4. Illustration of displacement at impact time for varying gauge sizes and waveforms.

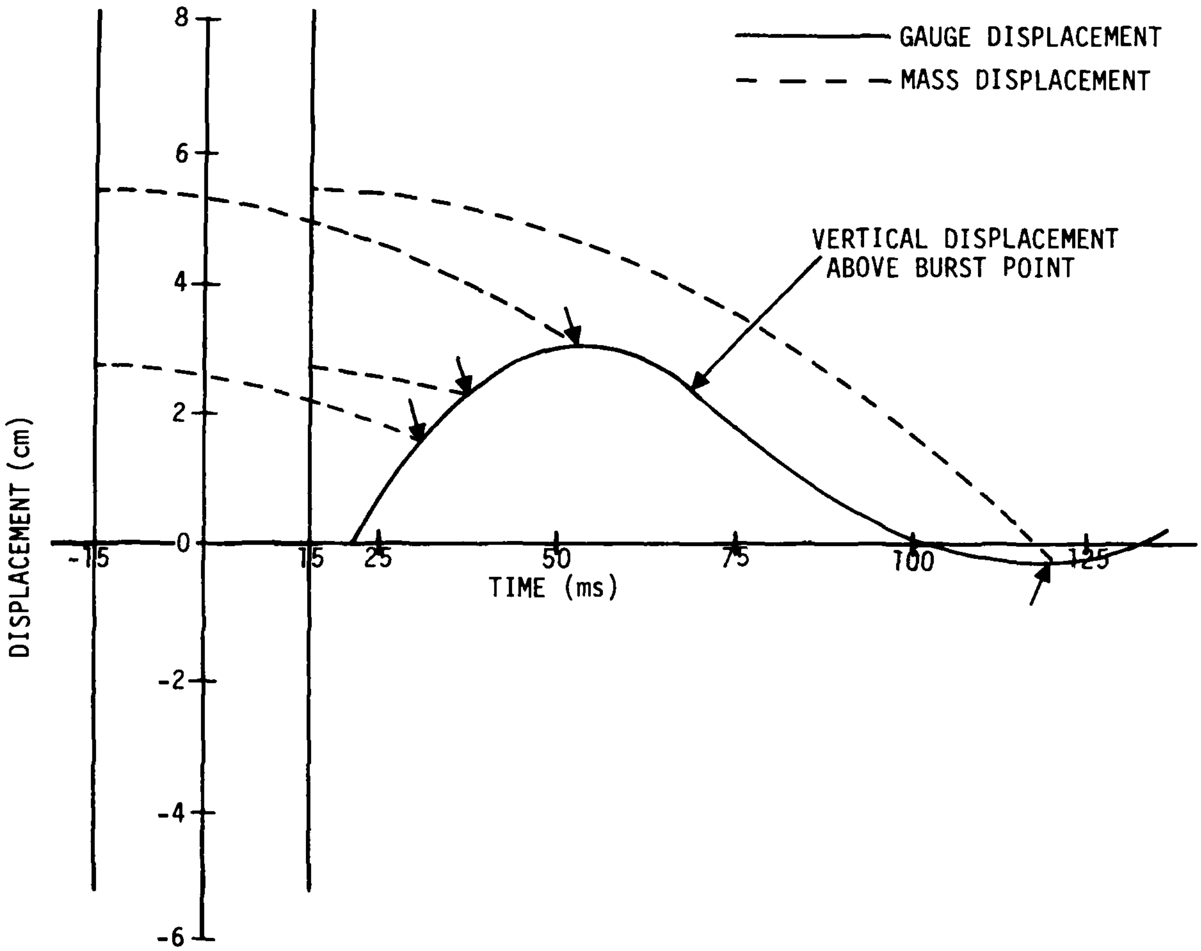

Figure 5. Effects of gauge size and weight-release time on recorded upward displacement.

d(t) at any time t must not exceed the free-fall position of the mass; namely,

$$d(t) \leq 1/2g(t - t_r)^2$$

Otherwise, the top of the gauge case would overtake the falling weight.

Several different modes of gauge operation will affect the measured displacement for downward motion. Figure 6 illustrates these cases. Traces of the particle motion of the top and bottom points of the gauge are shown.

- Curve A illustrates a case where the gauge overtakes the mass released at zero time, which would result in failure of the measurement.
- Curve B shows the effect of pre-release of the mass at -25 ms and for the same initial mass height of 2.54 cm. In this case, the weight trajectory does not intersect that of the gauge top.
- Curve C shows the effect of reducing the gauge size from 5 cm to 2.5 cm and pre-release of the weight at -50 ms.

(3) Problem with horizontal motion--Referring to Figure 1, the horizontal gauge displacement h is shown at position B. From the figure it can be seen that the maximum horizontal displacement at impact must be less than the initial distance to the gauge wall. Otherwise, the mass would strike the wall and interfere with the time-of-fall measurement. The horizontal dimensions then must be taken into account in the specific application of the gauge. Figure 7 illustrates the complicated particle motion below the ground surface from a surface burst. The gauge would require more than 5 cm

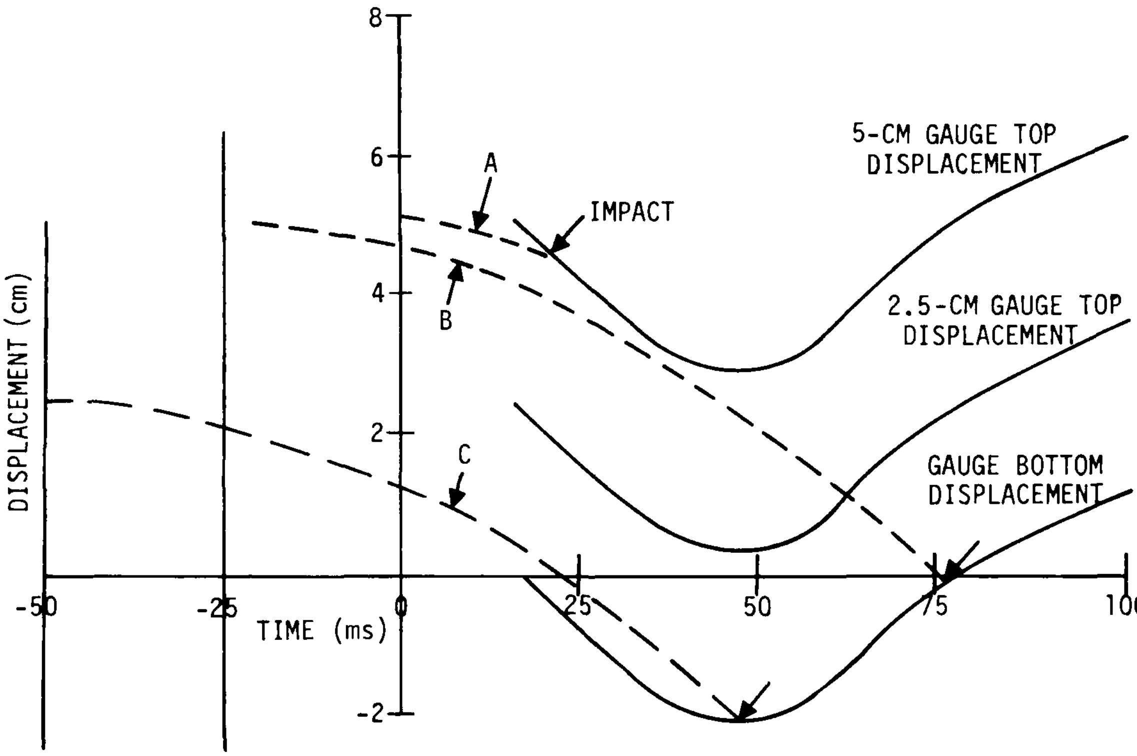

Figure 6. Effects of mass-release time and gauge size upon measured displacement of a downward vertical motion.

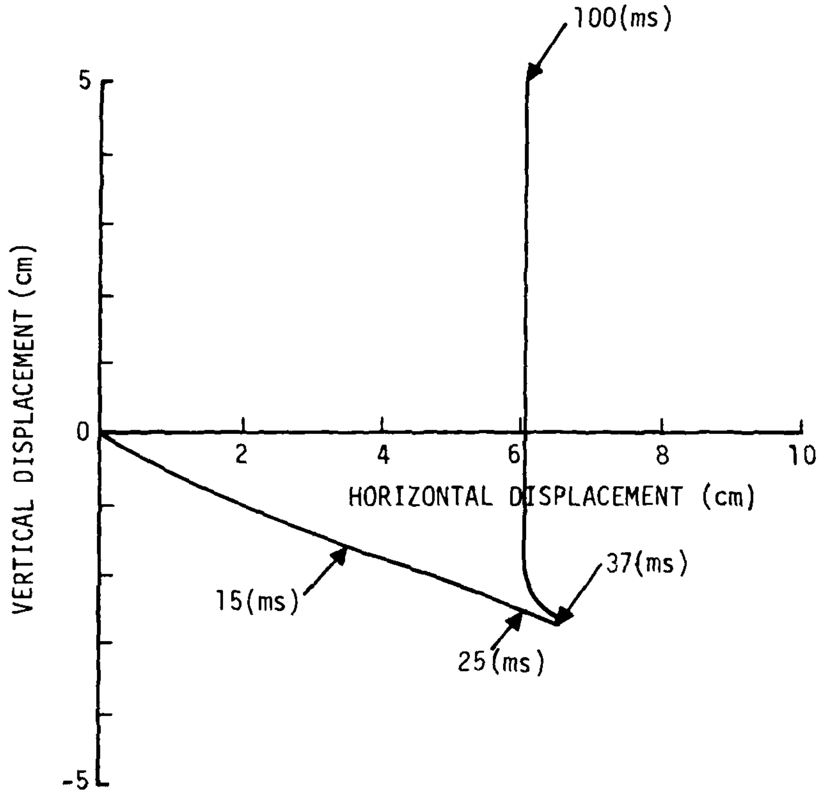

Figure 7. Particle displacement at 12-m range and 9-m depth below ground surface from a 500-ton surface burst.

horizontal clearance between the initial weight position and the gauge wall to record vertical motion to times greater than 37 ms.

(4) <u>Gauge case strength</u>--Mechanical hardening requirements for the displacement gauge may be greater than those for other types of ground-motion gauges. The large void required inside the gauge casing to accommodate the horizontal and vertical motions of the falling weight will increase the structural strength necessary to prevent buckling or crushing of the case prior to the measurement. The stress level at which a desired displacement measurement is to be made will depend upon the source yield and the peak displacement. All these factors must be taken into account in the design of the gauge housing. A great deal of experimental data on shock loading of cylindrical and other structures is available to estimate the structural hardening requirements or limitations for the design of the displacement gauge.

3. REVIEW OF ADVANTAGES AND DISADVANTAGES OF THE GAUGE DESIGN

These are some of the advantages associated with the gauge design described:

- No mechanical or electronic integration is required.
- There is an accurate inertial frame of reference (free fall).
- The data recorded includes only time-interval measurements, while amplitude measurements require calibration.
- Time-base drift is not possible.
- Time measurements of switch opening and closure provide high signal-to-noise ratio.

This gauge design does have certain disadvantages, such as:

- Only the vertical component of displacement is possible in the present gauge design.
- The dependence of gauge size upon magnitude of displacement requires careful estimates of expected ground motions.
- The time-squared dependence of free-fall distance imposes practical limitations on gauge size.

4. SOURCES OF ERROR IN MEASUREMENTS

Two possible effects on the accuracy of measurement are considered.

- Air drag on drop mass. Relative motion of the drop mass and the air enclosed in the gauge canister will induce air drag, which will oppose the free-fall motion of the weight. In Appendix B, this problem is analyzed with estimates of errors expected.
- Rotational motion effects on measurements. If the gauge motion undergoes a rotation, the effect on the measurement is to introduce an error in the measurement. In Appendix C, this effect is discussed.

III. DEVELOPMENT AND TESTS OF PROTOTYPE DISPLACEMENT GAUGE

1. GAUGE CONSTRUCTION

A prototype displacement gauge was built and tested by Systems, Science and Software at the Green Farm Test Facility in March 1974. Specific design features of the gauge were contributed by the author and Dr. Howard Kratz (formerly of Systems, Science and Software). Electronic circuitry design and laboratory testing were performed by Mr. William Muhl of IMED Corporation (Ref. 4). Figure 8 is an engineering sketch of the full-scale model with specific features of the gauge indicated.

a. Mass-release mechanism--The drop mass is supported by the copper wire under tension from the leaf spring. An electrical circuit (normally closed) is completed through the breakwire to the drop mass and mass support. On receiving a release signal, the solenoid is energized, breaking the wire which opens the electrical circuit and at the same time releases the drop mass. Opening of the circuit supplies an electrical timing signal of the mass release.

b. Foil switch--The foil switch, located at the bottom of the gauge case, consists of a copper foil insulated from the metal case by a mylar foil. An electrical circuit (initially open at the switch) is completed by the shorting pin attached to the drop mass, generating an electrical timing signal at impact.

c. Electrical circuitry--A block diagram of the electrical circuitry is shown in Figure 9. The mass-release delay circuit generates a signal prior to shock arrival at the gauge. Timing of the mass release could occur at or prior to detonation time, or be delayed depending upon the distance between the gauge and explosive charge.

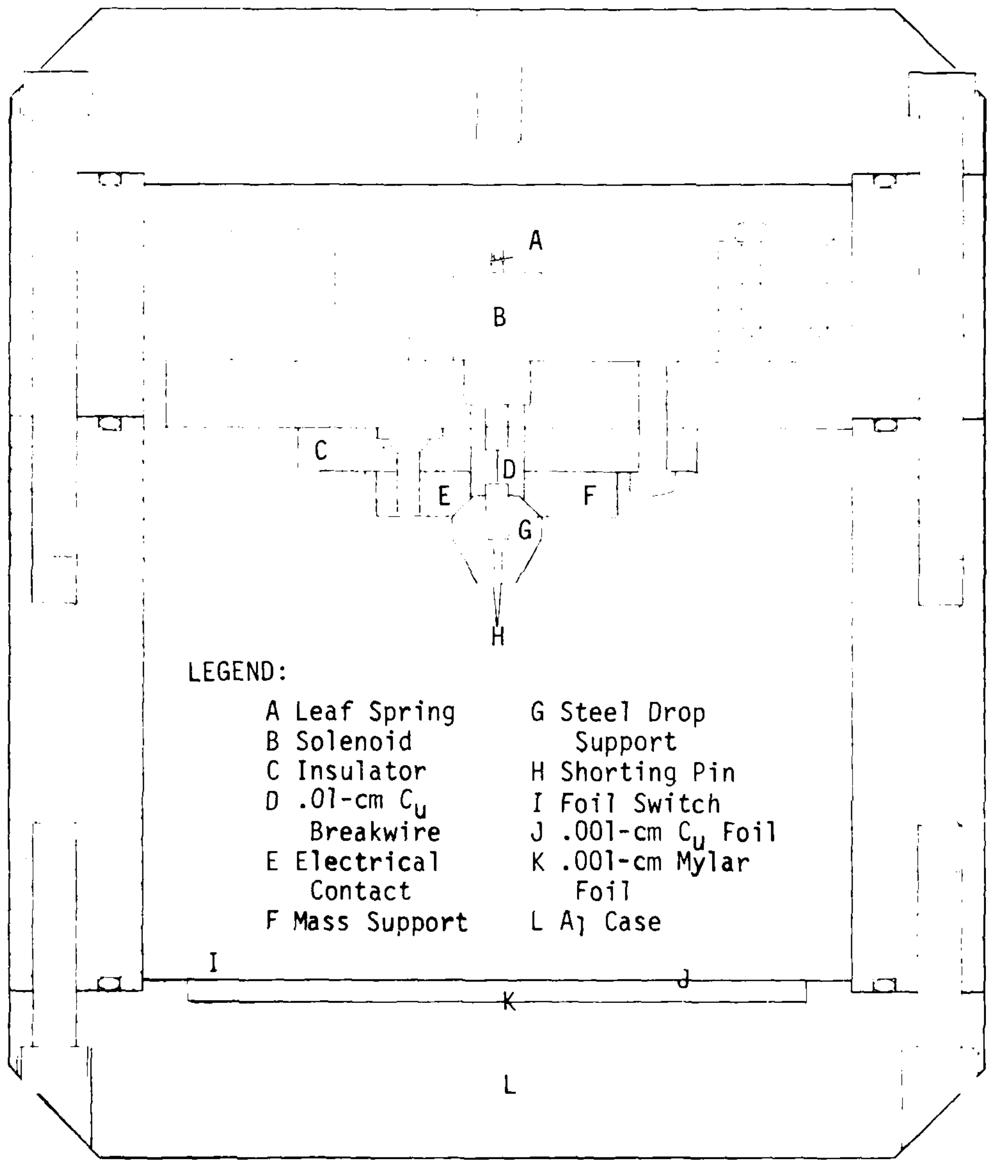

Figure 8 . Full-scale drawing of prototype ground-motion displacement gauge.

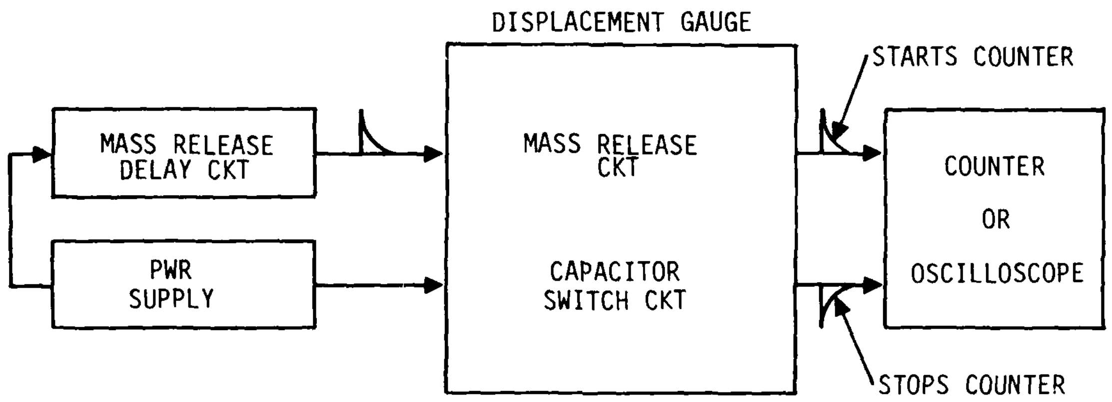

Figure 9. Block diagram of displacement gauge system.

The signal generated by the breakwire initiates the horizontal sweep of an oscilloscope, or can be used to start a counter. Arrival of the impact signal is recorded either on the oscilloscope or stops the counter if used. The time difference provides the time-of-fall from which the vertical displacement is calculated. Figure 10 is a schematic diagram showing the signal-generating circuits.

2. LABORATORY TESTS AND DISCUSSION OF RESULTS

During the MIGHTY MITE series of underground tests on seismic decoupling (Ref. 1), a test was planned that included the displacement gauge concept in the test program. That test was later cancelled; however, funding for construction and laboratory testing of the gauge was approved. Although no ground-motion displacement tests were attempted, gauge-displacement experiments were conducted to verify the gauge concept. Two sets of experiments are described and the results are presented in the following paragraphs.

a. Time-of-fall measurements--The first series of experiments simply consisted of measuring the free-fall time of the drop weight through an accurately measured drop distance with no motion of the gauge case. All the electronic circuits were energized as previously discussed. A trigger signal applied to the weight-release mechanism started an electronic counter with a time resolution of a few μsec. A signal at impact stopped the counter from which the time-of-fall was recorded. Table 1 summarizes these results obtained from the given drop distance. Also listed are the time differences from the calculated value, and the percentage differences. The consistency in the measurements would seem to indicate a systematic error either in the timing measurements or in the recorded drop distance. The difference between t_o and the mean is 2.0 ms.

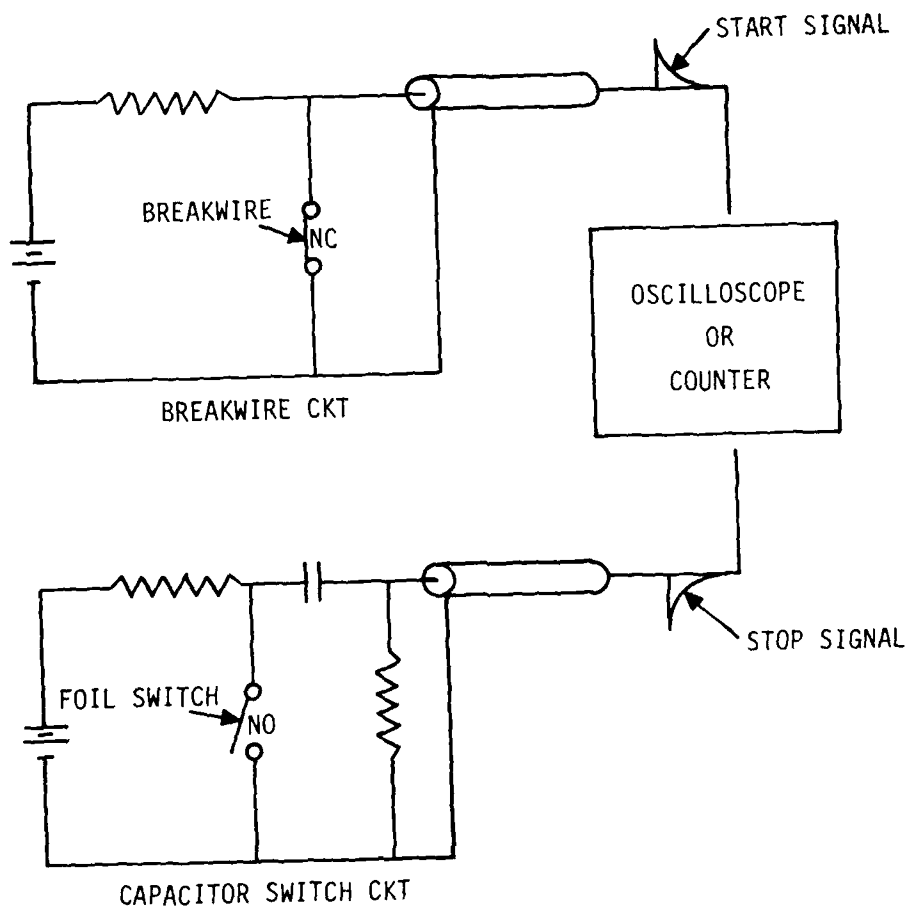

Figure 10. Schematic diagram of displacement gauge circuitry.

TABLE 1. FREE-FALL DROP-TEST MEASUREMENTS

Drop Distance S = 3.498 cm

Acceleration g = 980 cm/sec^2

Calculated Time-of-Fall t_o = 84.486 ms

TEST NO.	TIME-OF-FALL (ms)	$(t_o - t)$ms	% DIFF
1	82.52	1.967	2.32
2	82.64	1.845	2.18
3	82.21	2.276	2.69
4	82.70	1.786	2.11
5	82.69	1.796	2.13
6	82.60	1.886	2.23
7	82.22	2.266	2.68
8	82.09	2.396	2.84
	$\bar{t}$ = 82.46(ms) σ = 0.230(ms)		

b. <u>Gauge drop tests</u>--To simulate ground-motion displacement tests, the gauge was suspended a measured distance d_m above a bench top as shown in Figure 11. The gauge canister was released by firing of the HE detonator just after the drop mass was released. Measurements of time-of-fall t_m of the mass were recorded from which the apparent displacement was calculated by

$$d_a = S - 1/2gt_m^2$$

where S is the initial pin distance from the bottom of the gauge.

Table 2 summarizes the test results. The apparent displacements are significantly different from the displacements (gauge drop distances) measured prior to each test by more than 10 percent. Again, as noted in Table 1, the time-of-fall in each case is less than was predicted from the known displacement. Applying the correction of 2 ms from Table 1, the corrected percentages of difference in the displacements are reduced as shown in the last column of Table 2. These results do not determine the source of the apparent systematic error, and time did not permit further investigation of the problem. There is little reason to doubt that the accuracy of the measurements can be significantly improved by troubleshooting the weight release and impact timing.

TABLE 2. DROP-TEST MEASUREMENTS

$S = 5.08$ cm; $g = 980$ cm/sec^2

TEST NO.	t_m (ms)	d_m (cm)	d_a (cm)	% DIFF	% DIFF (corr)
1	123.575	2.774	2.403	13.4	4.58
2	123.294	2.703	2.368	12.5	3.36
3	122.060	2.530	2.220	12.2	2.70
4	125.090	2.891	2.5873	10.5	1.95

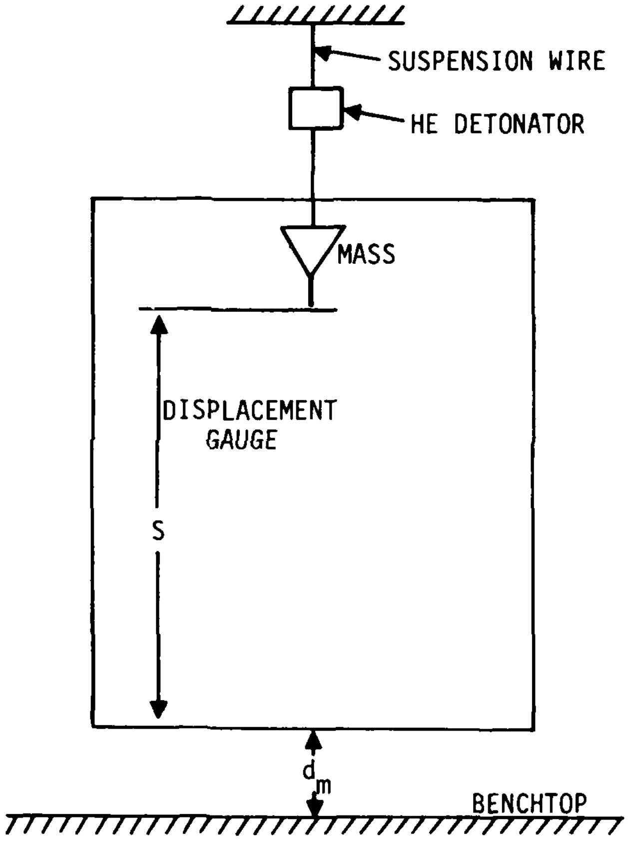

Figure 11. Experimental setup for simulation tests of displacement gauge.

IV. MODIFICATION OF GAUGE DESIGN FOR OTHER USES

1. PARTICLE VELOCITY

Measurement of particle velocity, in addition to particle displacement, would provide another data check on existing particle velocity gauges. The same principle of time-interval measurements is all that would be required using the concept that will be described in this section.

Figure 12 illustrates the concept. Two separate displacement gauges are contained within the same cannister as shown. Two drop masses and two impact switches would provide two near-displacement measurements separated by a small time interval. The spacing of the two measurements could be accomplished in either of two ways. Shorting pins of unequal length released simultaneously would provide two displacements. From Figure 12 the masses released at t_r would impact at times t_1 and t_2. The corresponding displacements are given by

$$d_1 = S_1 - 1/2g(t_1 - t_r)^2$$

$$d_2 = S_2 - 1/2g(t_2 - t_r)^2,$$

from which the average velocity over the displacement interval is obtained:

$$\bar{u} = \frac{d_2 - d_1}{t_2 - t_1} .$$

Figure 13 illustrates the principle of velocity measurement. Two different displacement curves are shown to illustrate positive and negative velocity measurements.

The second method works basically in the same manner where the two masses are released at different times,

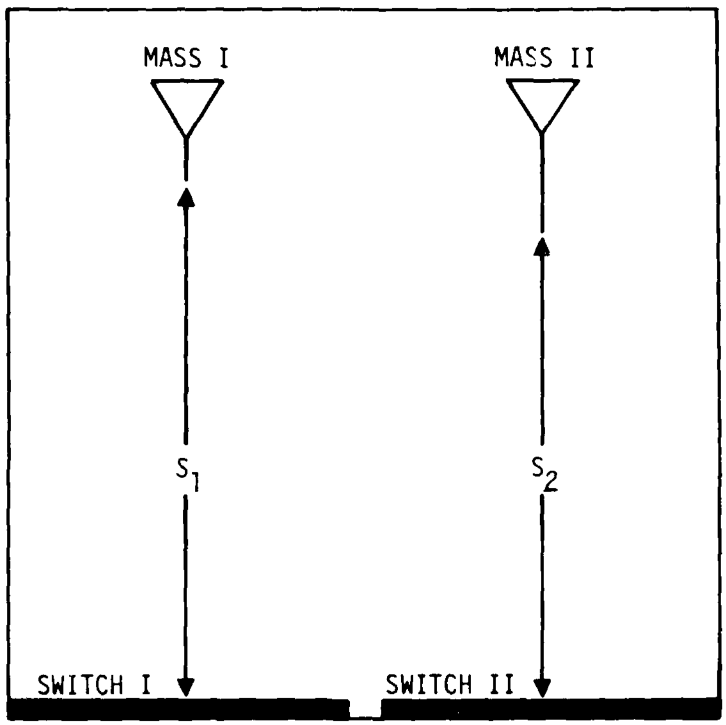

Figure 12. Modified displacement velocity gauge.

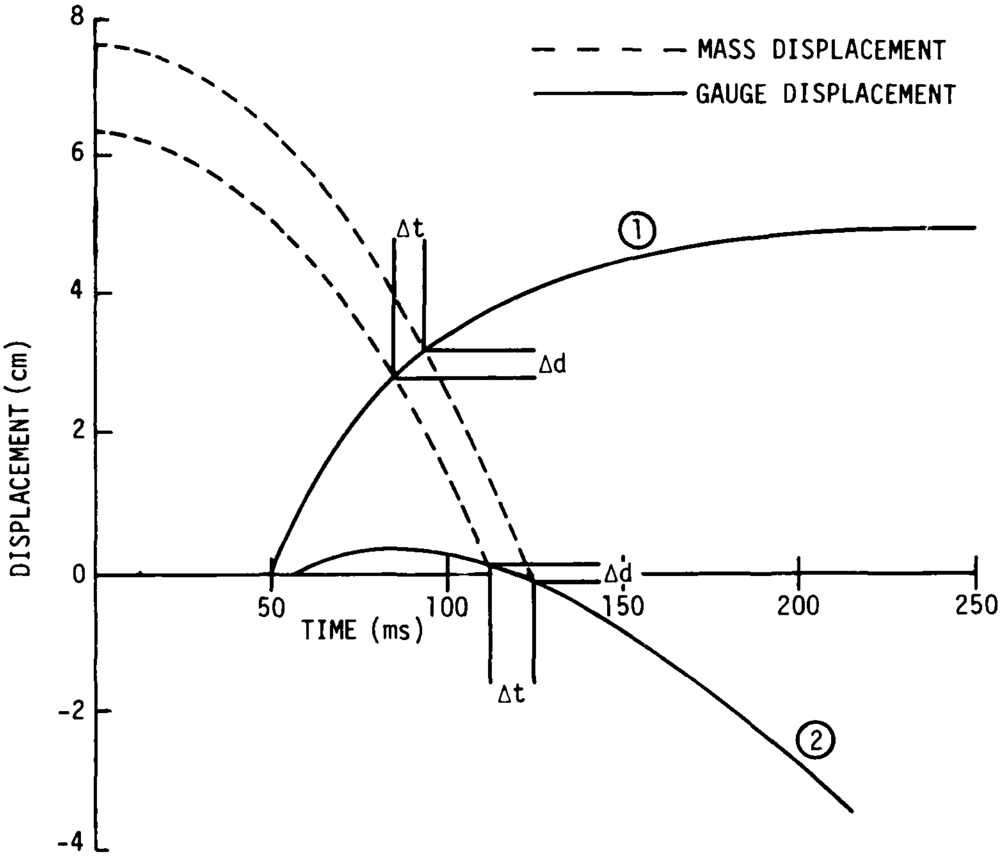

Figure 13. Particle velocity obtained from displacement measurements.

t_1 and t_2, with impact times t_3 and t_4, respectively. The displacements are obtained from

$$d_1 = S - 1/2g(t_3 - t_1)^2$$

$$d_2 = S - 1/2g(t_4 - t_2)^2$$

and the velocity calculated from

$$\bar{u} = \frac{d_2 - d_1}{t_4 - t_3} .$$

2. HORIZONTAL AND VERTICAL DISPLACEMENT

Another possible application of the gauge concept is the measurement of the horizontal and vertical components of permanent displacement. Only the vertical component can be measured using the basic design as illustrated in Figure 1. The horizontal motion could be inferred from the vertical measurement in the case of known spherical symmetry along a given radial direction.

A gauge of special design, used in conjunction with the basic model, could in principle be used to determine both components of permanent displacement. Figure 14 is an illustration of the dual gauge principle where Gauge I has been modified by constructing the foil switch in the form of a cone as shown. Gauge II is the basic design discussed throughout the report. Operation of the system is as follows: at 'zero time' both weights are released at a distance S from the common base BB. The gauge undergoes a final upward displacement D, with horizontal and vertical components H and V as shown. Impacts of the masses at P_1 and P_2 occur at times t_1 and t_2 respectively, with the base now located at B'B'. Motions of the drop masses at impact are given by

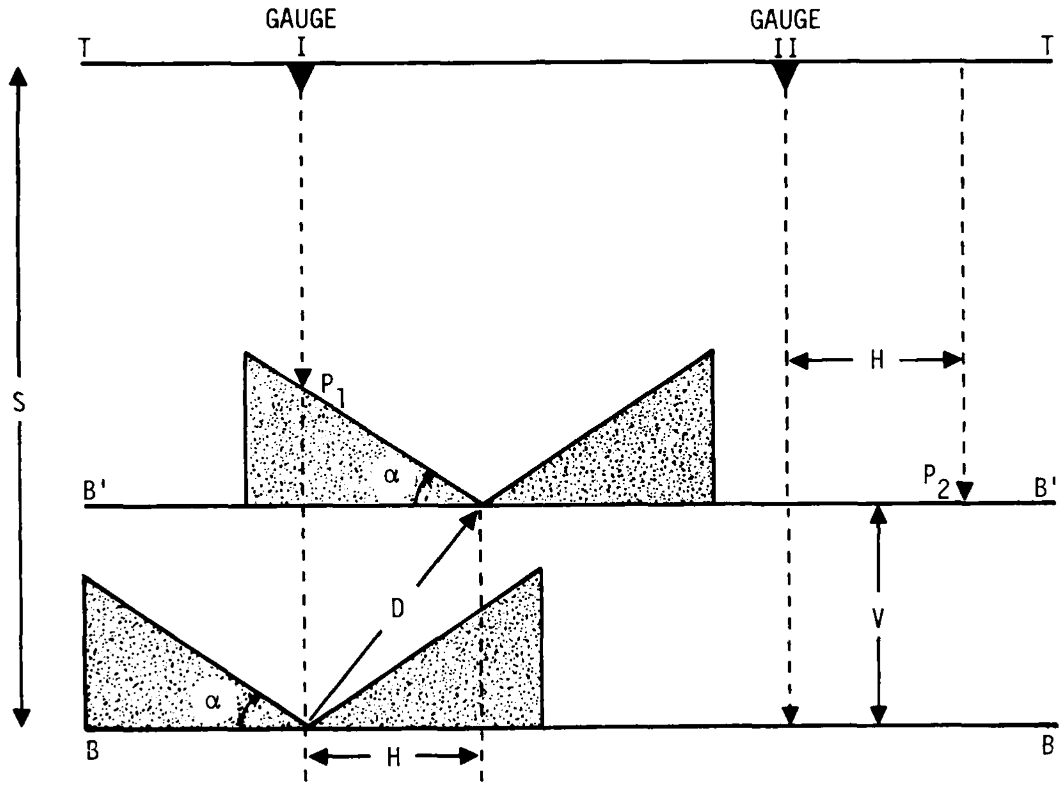

Figure 14. Schematic illustration of technique to measure horizontal and vertical displacement.

$$1/2gt_1^2 = S - V - H\tan\alpha$$

$$1/2gt_2^2 = S - V,$$

hence,

$$1/2g\left(t_2^2 - t_1^2\right) = H\tan\alpha,$$

where α is the angle subtended from the horizontal by the conical foil switch. The displacement can then be calculated to be

$$H = 1/2g\left(t_2^2 - t_1^2\right)/\tan\alpha$$

$$V = S - 1/2gt_2^2$$

It should be noted that this technique can only be used for a final displacement since, in the case of a transient measurement, two different displacements would occur at times t_1 and t_2, which would not uniquely determine these displacements.

V. VERIFICATION TESTS OF ACCELEROMETER AND VELOCITY GAUGES

More recently, another application has been suggested. Particularly with the increase in the application of high explosives for the simulation of nuclear explosions, the gauge can be an important tool in calibrating ground-motion measurements.

Ground-motion displacement is generally obtained either by double time-integration of acceleration data or single time-integration of particle velocity data. This has been the case since no completely satisfactory displacement gauge has been developed. The measurement of particle displacement poses a difficult problem in devising schemes for direct measurement, since a fixed-reference position is required to determine the relative displacement. However, the methods using integration of acceleration and particle velocity data often introduce errors in the calculated displacement. The reference voltage or signal output from a gauge may vary with time (baseline shift) which introduces a cumulative error of unknown value in the displacement obtained by integration. The total signal consists of the real signal superimposed upon the varying reference base. Figure 15 illustrates the different ground displacement results obtained from actual time-integrated accelerometer and particle velocity data. Both gauges were contained in the same instrumentation package. The solid curve shows the results from the acceleration data which have been singly integrated to obtain the particle velocity and doubly integrated to yield displacement. The dotted curve is a record of the velocity measurement and its integration to obtain displacement. These results show the necessity for a method to measure displacement at a point to determine the discrepancy in the measurements.

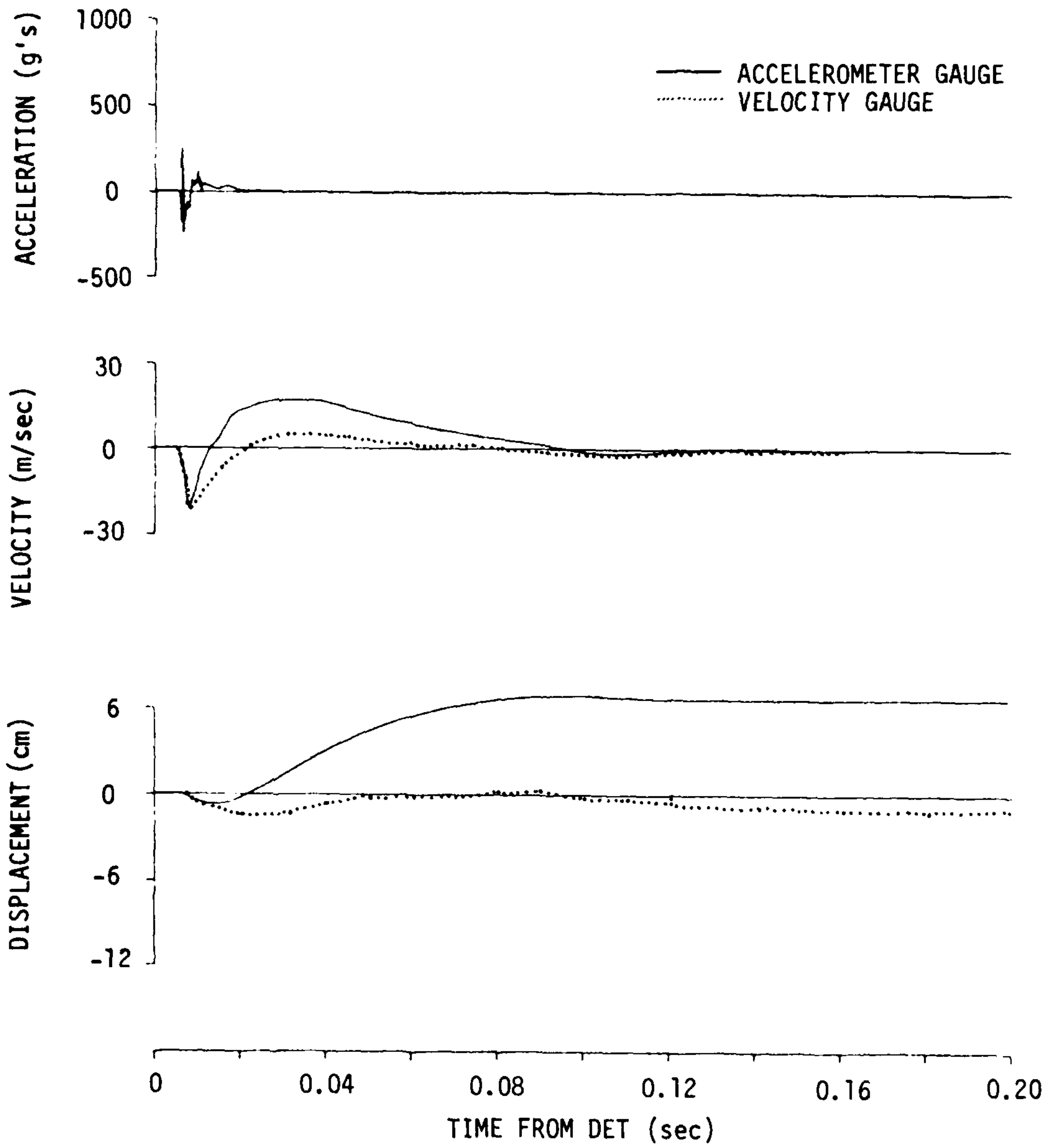

Figure 15. Ground motions vs time, Mineral Rock Gauge 60-18.

REFERENCES

1. Whitener, J. E., Proposed Test Program to Study Mechanisms Involved in Enhanced Cavity Decoupling, R & D Associates, RDA-TR-075-DNA, May 1972.

2. Whitener, J. E., MIGHTY MINE Series, (a) DIAMOND DUST Event , (Unpublished); (b) DIAMOND MINE Event (Unpublished); (c) PRE-MINE DUST Event, POR 6822, March 1975; Technical Directors Summary Reports, Defense Nuclear Agency.

3. Latter, A. L., et al., A Method of Concealing Underground Nuclear Explosions," The RAND Corporation, RM-2347, March 1959.

4. Muhl, W., Laboratory Research Note Book, Systems, Science and Software, March 1974.

5. White, J. E., Seismic Waves: Radiation, Transmission, and Attenuation, McGraw-Hill, 1965.

APPENDIX A. DISPLACEMENT POTENTIAL

From the theory of elasticity, the permanent elastic displacement of the cavity wall is related to the energy released by an explosion given by

$$\frac{4\pi}{3} \frac{Pa^3}{\gamma-1} = \frac{16\pi\mu a^2 d_a}{3(\gamma-1)}$$

where $p \equiv$ cavity pressure,

$\mu \equiv$ shear modulus of medium,

$a \equiv$ radius of the cavity,

$d_a \equiv$ permanent wall displacement.

With the approximation of incompressible flow,

$$a^2 d_a = r^2 d_r ,$$

the effective energy released in the cavity becomes

$$\frac{4\pi}{3} \frac{Pa^3}{\gamma-1} = \frac{16\pi\mu r^2 d_r}{3(\gamma-1)}$$

The constant r^2d is often referred to as the displacement potential. Figure A1 shows the displacement produced by a step-pressure applied to a cavity wall (Ref. 5). The static part of the solution becomes evident at late times. Also shown is the permanent displacement which would be measured by the technique discussed in the report.

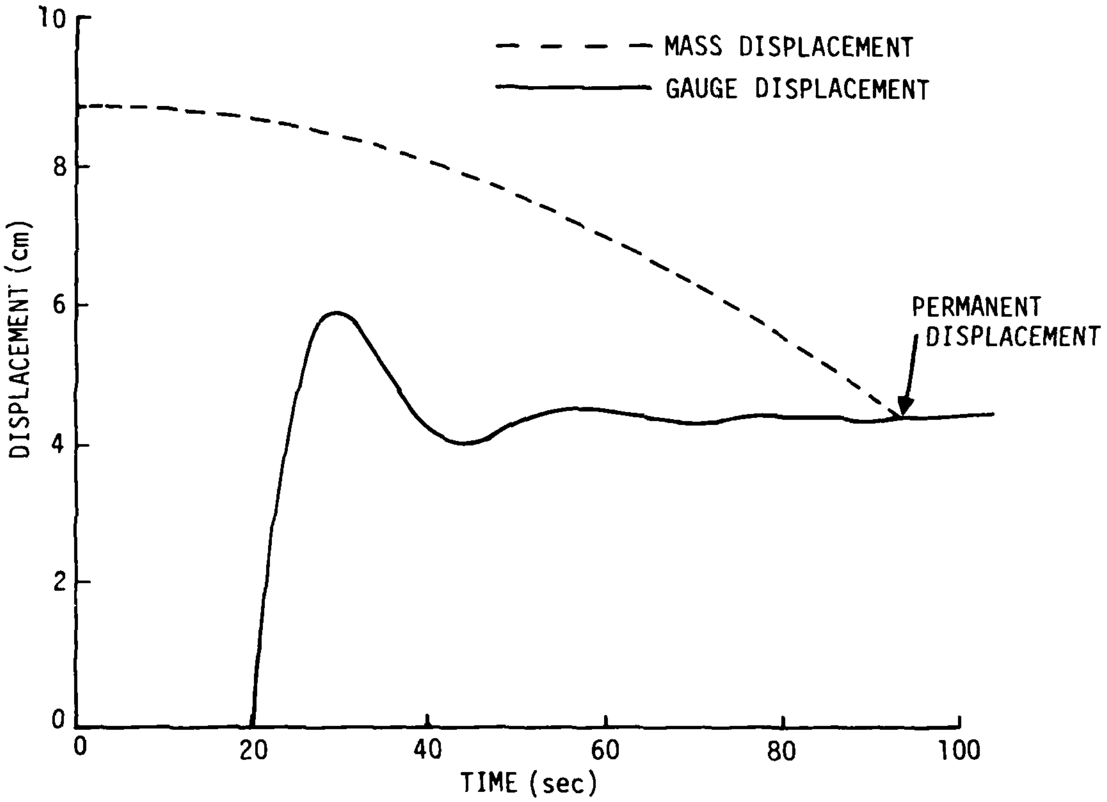

Figure A1. Displacement potential obtained from permanent-displacement measurement.

APPENDIX B. EFFECTS OF AIR DRAG ON DISPLACEMENT MEASUREMENTS

The relative motion of the drop mass and the air inside the gauge case will apply a drag force opposing the free-fall motion of the weight. In the case of an upward displacement, the flow velocity over the mass will be the ground particle velocity superimposed upon the instantaneous mass velocity. The net force per-unit-area acting on the mass is given by

$$F = 1/2\rho_a (U_p - U)^2 C_d - mg \qquad (B1)$$

where m = mass per-unit-area of mass,
C_d = drag coefficient,
U_p = gauge case velocity,
U = mass velocity,
ρ_a = air density.

This additional force will affect the time-to-impact and an error in the computed displacement will result. In this Appendix, the error in displacement due to the air drag is estimated.

a. Assumptions--The equations of motion of the mass can be solved using Eq. (B1) when U_p is known; however, the solutions are quite complicated except for special cases. Several simplifying, conservative assumptions will be made and justified by the results. These assumptions are:

- The particle velocity U_p is a step function equal to the peak velocity.
- The drag coefficient $C_d = 1$.
- The relative velocity $(U_p + U_o)$ is constant over the motion where U_o is the maximum free-fall velocity in vacuum, $U_o = \sqrt{2Sg}$.
- The mass = 10 gm/cm^2.

All of the assumptions are overestimates which will provide an upper bound on the displacement error.

b. Equations of motion--Under these assumptions, the net force F will be constant over the motion, which will be free-fall with an apparent acceleration g' obtained from Eq. B1:

$$g' = g \left(1 - \frac{1/2\rho_a (U_p - U_o)^2 C_d}{mg}\right) . \qquad \text{(B2)}$$

The calculated displacement for the measured time-of-fall t_m then becomes

$$d_c = S - 1/2 g' t_m^2 , \qquad \text{(B3)}$$

and the displacement in the absence of air drag is given by

$$d = S - 1/2 g t^2 . \qquad \text{(B4)}$$

Since

$$d_c = U_p t_m \qquad \text{(B5)}$$

and

$$d = U_p t , \qquad \text{(B6)}$$

the fractional displacement error can be written

$$e = \frac{d - d_c}{d} = \frac{t - t_m}{t} \qquad \text{(B7)}$$

where t, t_m can be obtained by substituting d, d_c from Eqs. (B5) and (B6) into Eqs. (B3) and (B4) respectively, and solving for t, t_m:

$$t_m = \frac{U_p}{g'}\left(\sqrt{1 + 2Sg'/U_p^2} - 1\right) \qquad \text{(B8)}$$

$$t = \frac{U_p}{g}\left(\sqrt{1 + 2Sg/U_p^2} - 1\right) \qquad \text{(B9)}$$

where $U_o + U_p$ in Eq. B2 is given by

$$U_o + U_p = U_p\left(1 + \sqrt{2gS/U_p^2}\right)$$

to obtain g'. The parameters in the problem are the gauge size S and the vertical particle or gauge case velocity U_p, which will be varied in the displacement error computations.

c. Calculations of displacement error--Table B1 shows values of errors obtained by solving Eqs. (B8) and (B9) using the values of S and U_p listed in the table. These values probably cover the range for any practical application of the displacement gauge.

The results show that the drag effects are small for the very conservative approximations used in the computations. There are compensating effects which reduce the error. As the particle velocity increases, the drag also increases; however, the time-to-impact decreases, which tends to reduce the drag impulse on the mass.

TABLE B1. PERCENTAGE ERRORS IN DISPLACEMENT DUE TO AIR DRAG

S (cm)	U_p (cm/sec)			
	10	100	1,000	10,000
2	0.01	0.01	0.01	0.01
5	0.03	0.04	0.02	0.02
10	0.07	0.08	0.04	0.03
20	0.14	0.16	0.09	0.07
30	0.20	0.24	0.14	0.10

APPENDIX C. ERROR DUE TO ROTATIONAL MOTION

Throughout the report in the discussion on the operation of the displacement gauge, it has been assumed that gauge motion was purely translational without rotation. However, a gauge imbedded in a heterogeneous medium or in a region of tectonic stress could undergo a rotation superimposed upon its linear motion.* In addition, gravity can also introduce rotational motion of the field of flow. In this appendix, the error produced in vertical displacement measurements due to rotational motion is analyzed.

In Figure C1, the initial position of the gauge is shown with the base located along AA. Impact of the mass at P would occur for a vertical displacement V in the absence of rotation. A rotational motion is assumed for a constant radius of curvature r through the angle θ to the new base position BB. The motion results in a point of impact at P' with an apparent vertical displacement V'. Also, the rest point P_o is displaced horizontally by H. The error in the vertical displacement with rotation is defined as the fractional difference between the apparent displacement and the true displacement, namely,

$$E = \frac{V' - V}{V}$$

From Figure C1 it can be shown that

$$V' = r\tan\theta$$
$$V = r\sin\theta$$

*Personal communication between the author and G. Rawson (Consultant, RDA).

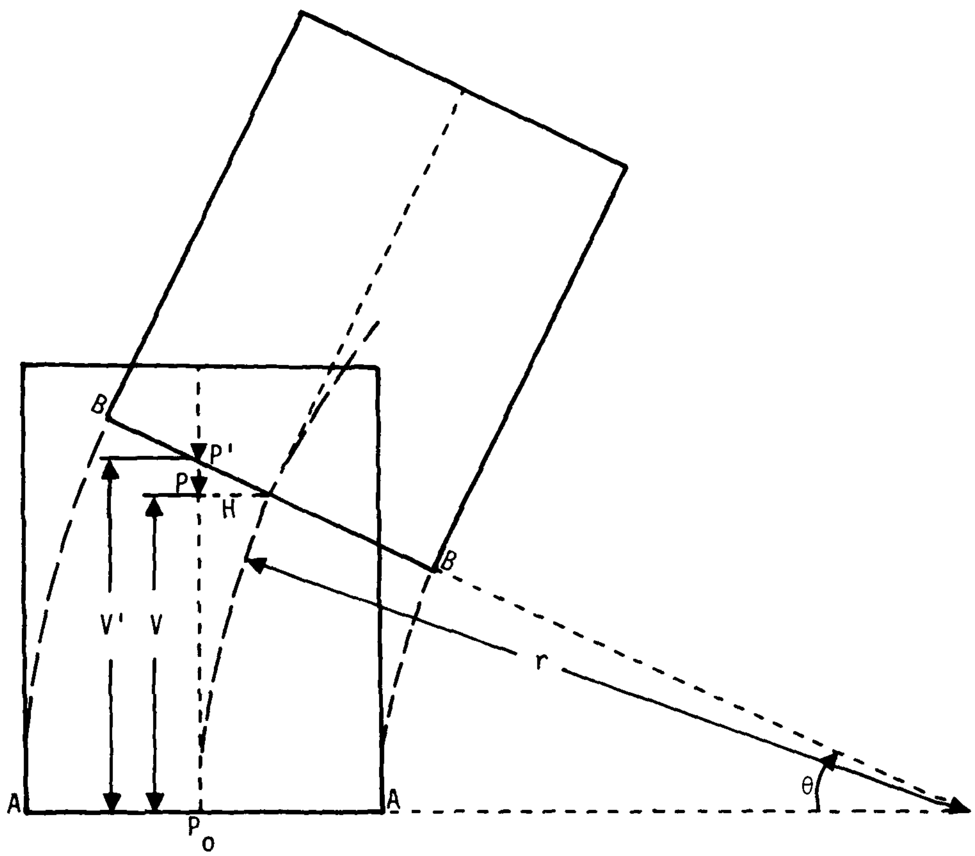

Figure C1. Illustration of effects on ground-motion displacement measurements due to rotational motion.

Hence,

$$\frac{V' - V}{V} = \frac{1 - \cos\theta}{\cos\theta}$$

A plot of the percentage difference between the apparent and true vertical displacements is shown in Figure C2. It is interesting to note that the error is independent of r, the radius of curvature. Displacements of interest are expected to be small compared to the radius of curvature in rotational motion, hence the angle of rotation would be correspondingly small. Angular motions to 20 deg produce small errors, as noted in Figure C2.

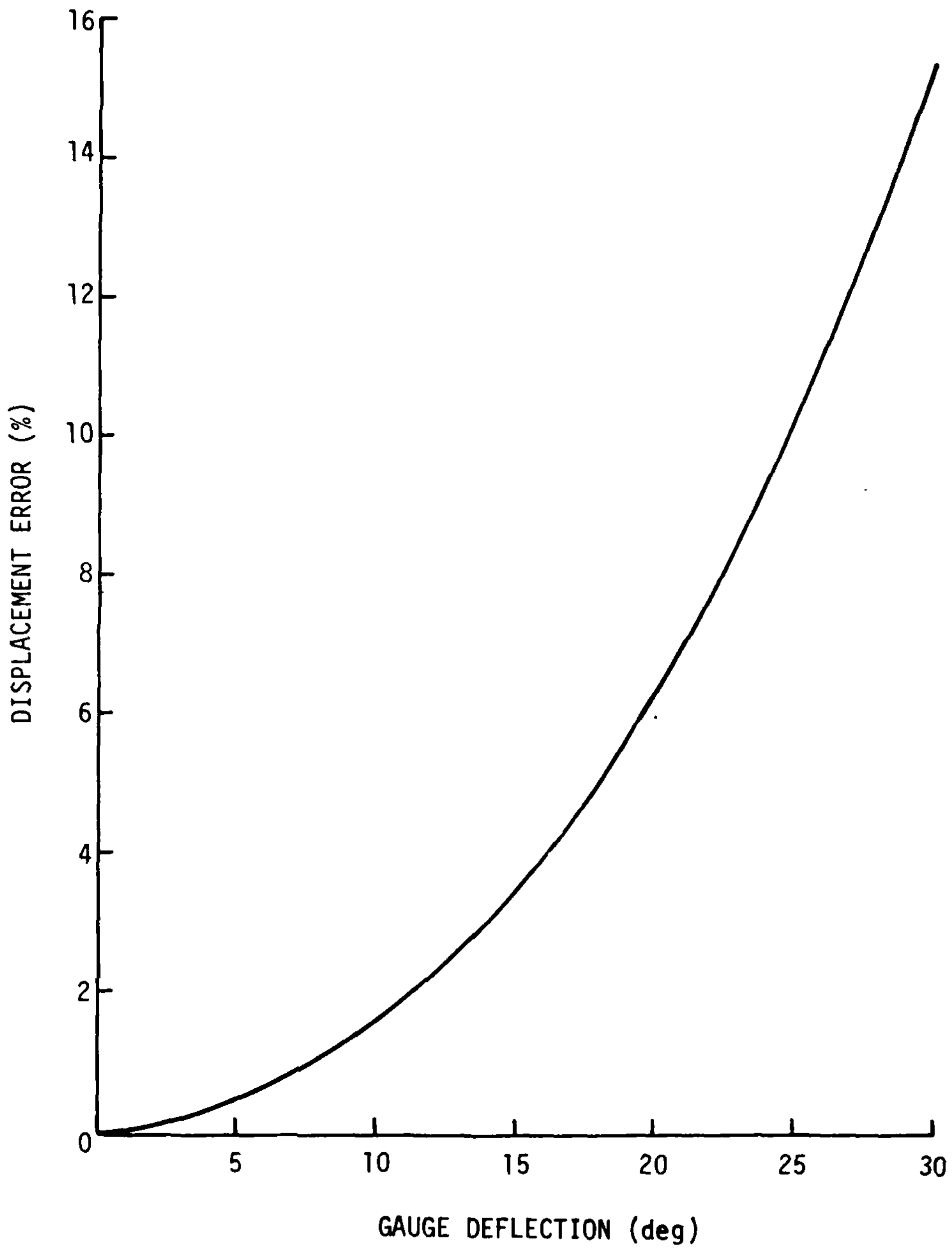

Figure C2. Displacement error due to gauge rotation.

DISTRIBUTION LIST

DEPARTMENT OF DEFENSE

Assistant to the Secretary of Defense
Atomic Energy
ATTN: Executive Assistant

Defense Intelligence Agency
ATTN: DB-4C, E. O'Farrell
ATTN: DT-1C
ATTN: DT-2

Defense Nuclear Agency
2 cy ATTN: SPSS
4 cy ATTN: TITL

Defense Technical Information Center
12 cy ATTN: DD

Department of Defense Explo Safety Board
ATTN: Chairman

Field Command
Defense Nuclear Agency
ATTN: FCT
ATTN: FCPR
ATTN: FCTMOF

Field Command
Defense Nuclear Agency
Livermore Branch
ATTN: FCPRL

Field Command Test Directorate
Defense Nuclear Agency
ATTN: FCTC

NATO School (SHAPE)
ATTN: U.S. Documents Officer

Under Secretary of Def for Rsch & Engrg
ATTN: Strategic & Space Sys (OS)

DEPARTMENT OF THE ARMY

Chief of Engineers
Department of the Army
ATTN: DAEN-MCE-D
ATTN: DAEN-RDL

Harry Diamond Laboratories
Department of the Army
ATTN: DELHD-N-P
ATTN: 00100 Commander/Tech Dir/TSO

U.S. Army Ballistic Research Labs
ATTN: DRDAR-BLT, J. Keefer
ATTN: DRDAR-TSB-S
ATTN: DRDAR-BLV
ATTN: DRDAR-BLT, W. Taylor

U.S. Army Concepts Analysis Agency
ATTN: CSSA-ADL

U.S. Army Material & Mechanics Rsch Ctr
ATTN: Technical Library

DEPARTMENT OF THE ARMY (Continued)

U.S. Army Engr Waterways Exper Station
ATTN: WESSD, J. Jackson
ATTN: J. Strange
ATTN: Library
ATTN: WESSA, W. Flathau

U.S. Army Materiel Dev & Readiness Cmd
ATTN: DRXAM-TL

U.S. Army Missile Command
ATTN: RSIC

U.S. Army Mobility Equip R&D Cmd
ATTN: DRDME-WC

U.S. Army Nuclear & Chemical Agency
ATTN: Library

XVIII Airborne Corps
Department of the Army
ATTN: F. Ford

DEPARTMENT OF THE NAVY

David Taylor Naval Ship R&D Ctr
ATTN: Code 1844
ATTN: Code 17
ATTN: Code L42-3
2 cy ATTN: Code 1740.5, B. Whang

Naval Civil Engineering Laboratory
ATTN: Code L08A
ATTN: Code L51, J. Crawford
ATTN: L51, R. Murtha

Naval Electronic Systems Command
ATTN: PME 117-21

Naval Facilities Engineering Command
ATTN: Code 04B

Naval Material Command
ATTN: MAT 08T-22

Naval Research Laboratory
ATTN: Code 8440, G. O'Hara
ATTN: Code 2627

Naval Sea Systems Command
ATTN: SEA-0351
ATTN: SEA-09G53
ATTN: SEA-0322

Naval Surface Weapons Center
ATTN: Code R14, I. Blatstein
ATTN: Code F31
ATTN: Code R14

Naval Surface Weapons Center
ATTN: Tech Library & Info Svcs Br

Office of Naval Research
ATTN: Code 474, N. Perrone

DEPARTMENT OF THE NAVY (Continued)

Office of the Chief of Naval Operations
ATTN: OP 03EG
ATTN: OP 981

Strategic Systems Project Office
Department of the Navy
ATTN: NSP-43
ATTN: NSP-272

DEPARTMENT OF THE AIR FORCE

Air Force Geophysics Laboratory
ATTN: LWW, K. Thompson

Air Force Institute of Technology
ATTN: Library

Air Force Systems Command
ATTN: DLW

Air Force Weapons Laboratory
Air Force Systems Command
ATTN: NTE, M. Plamondon
ATTN: NTES-C, R. Henny
ATTN: SUL
ATTN: DEX

Air University Library
Department of the Air Force
ATTN: AUL-LSE

Assistant Chief of Staff
Intelligence
Department of the Air Force
ATTN: INT

Deputy Chief of Staff
Research, Development, & Acq
Department of the Air Force
ATTN: AFRDQI

Strategic Air Command
Department of the Air Force
ATTN: NRI, STINFO Library

DEPARTMENT OF ENERGY

Department of Energy
Albuquerque Operations Office
ATTN: CTID

Department of Energy
ATTN: OMA/RD&T

Department of Energy
Nevada Operations Office
ATTN: Mail & Rec for Tech Lib

OTHER GOVERNMENT AGENCIES

Central Intelligence Agency
ATTN: OSWR/NED

Federal Emergency Management Agency
ATTN: Assistant Associated Dir

DEPARTMENT OF ENERGY CONTRACTORS

Lawrence Livermore National Lab
ATTN: Technical Info Dept Library

Los Alamos National Scientific Lab
ATTN: MS 364
ATTN: MS 670, J. Hopkins

Sandia National Laboratories
Livermore Laboratory
ATTN: Lib & Sec Class Div

Sandia National Lab
ATTN: 3141

DEPARTMENT OF DEFENSE CONTRACTORS

Aerospace Corp
ATTN: Technical Information Services

Applied Research Associates, Inc
ATTN: N. Higgins
ATTN: J. Bratton

BDM Corp
ATTN: T. Neighbors
ATTN: Corporate Library

Boeing Co
ATTN: Aerospace Library

California Research & Technology, Inc
ATTN: M. Rosenblatt

California Research & Technology, Inc
ATTN: D. Orphal

EG&G Wash Analytical Svcs Ctr, Inc
ATTN: Library

Electromech Sys of New Mexico, Inc
ATTN: L. Piper

Electromech Sys of New Mexico, Inc
ATTN: R. Shunk

Eric H. Wang
Civil Engineering Rsch Fac
ATTN: N. Baum

Geocenters, Inc
ATTN: E. Marram

H-Tech Labs, Inc
ATTN: B. Hartenbaum

IIT Research Institute
ATTN: Documents Library

Institute for Defense Analyses
ATTN: Classified Library

JAYCOR
ATTN: H. Linnerud

DEPARTMENT OF DEFENSE CONTRACTORS (Continued)

Kaman Sciences Corp
ATTN: Library

Kaman Tempo
ATTN: DASIAC

Lockheed Missiles & Space Co, Inc
ATTN: T. Geers
ATTN: Technical Library

Lockheed Missiles & Space Co, Inc
ATTN: TIC, Library

Lovelace Biomedical & Environmental Rsch Inst, Inc
ATTN: D. Richmond

Martin Marietta Corp
ATTN: G. Freyer

University of New Mexico
ATTN: CERF, N. Baum
ATTN: CERF, G. Leigh

Pacific-Sierra Research Corp
ATTN: H. Brode

Pacifica Technology
ATTN: G. Kent

Physics Applications, Inc
ATTN: F. Ford

Physics International Co
ATTN: Technical Library
ATTN: F. Sauer
ATTN: E. Moore

R & D Associates
ATTN: R. Port
ATTN: Technical Information Center
ATTN: J. Lewis
ATTN: P. Haas
4 cy ATTN: J. Whitener

DEPARTMENT OF DEFENSE CONTRACTORS (Continued)

Science Applications, Inc
ATTN: J. Dishon

Science Applications, Inc
ATTN: Technical Library

Science Applications, Inc
ATTN: J. Cockayne
ATTN: W. Layson
ATTN: M. Knasel

Southwest Research Institute
ATTN: W. Baker
ATTN: A. Wenzel

SRI International
ATTN: G. Abrahamson
ATTN: B. Gasten

Systems, Science & Software, Inc
ATTN: Library
ATTN: D. Grine

TRW Defense & Space Sys Group
ATTN: D. Baer
ATTN: Technical Information Center
2 cy ATTN: N. Lipner

TRW Defense & Space Sys Group
ATTN: P. Dai
ATTN: E. Wong

Weidlinger Assoc, Consulting Engineers
ATTN: M. Baron

Weidlinger Assoc, Consulting Engineers
ATTN: J. Isenberg

Weidlinger Assoc, Consulting Engineers
ATTN: A. Misovec

Blank

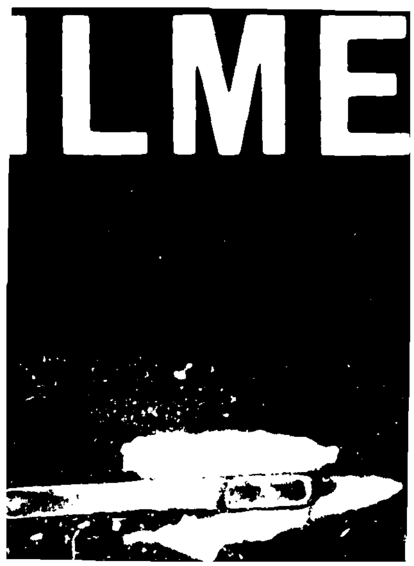
ILME